ELSEVIER

Surface Science 361/362 (1996) 537–541

surface science

# Electron–phonon scattering rates in GaAs/AlGaAs 2DEG samples below 0.5 K

A. Mittal [a,*], R.G. Wheeler [a], M.W. Keller [a,1], D.E. Prober [a], R.N. Sacks [b,2]

[a] *Departments of Applied Physics and Physics, Yale University, New Haven, CT 06520-8284, USA*
[b] *United Technologies Research Center, East Hartford, CT 06108, USA*

Received 21 June 1995; accepted for publication 1 November 1995

**Abstract**

We have studied electron heating in a 2DEG in GaAs/AlGaAs heterojunctions below 0.5 K. The electron temperature was raised above the lattice temperature using Joule heating. Weak localization and the temperature-dependent sample resistance were used as thermometers for the electrons. The electron–phonon energy relaxation rate was found to be proportional to $T^3$. We find that the relaxation rate increases with disorder in the system.

## 1. Introduction

Electron–phonon scattering is one of the fundamental processes in solids. Although well characterized in clean bulk metals, the understanding in lower-dimensional and in disordered systems is limited. Studies in metal films are complicated by issues of film purity, film thickness, and effects of substrate coupling [1]. A two-dimensional electron gas (2DEG) formed at the interface of a lattice-matched heterostructure from electrons in the lowest quantized subband offers a cleaner system to study this interaction, because the issues of phonon dimensionality and non-sphericity of the Fermi surface do not pose a problem. One can then study just the effect of disorder on electron–phonon scattering.

We present an experimental study of electron–phonon interaction time $\tau_{e\text{-}ph}$ below 0.5 K in a 2D electron gas in GaAs/AlGaAs heterostructures. Apart from being a fundamental quantity in itself, the energy relaxation rate is also relevant to studies of novel phenomena which occur only at low temperatures.

Most investigations of $\tau_{e\text{-}ph}$ are based on one of the following two kinds of experiments. The first relies on weak localization to extract the phase-breaking rate [2]. At high temperatures, the phase-breaking rate is approximately the electron–phonon scattering rate [3]. However, at low temperatures, electron–electron dephasing dominates. The second technique uses electron heating, and is sensitive only to energy relaxation mechanisms. Power dissipated in the electron gas heats it up above the phonon temperature $T_{ph}$. In long samples, the temperature rise is proportional to $\tau_{e\text{-}ph}$ for small powers. At low temperatures, electron out-diffusion can provide a competing mechanism for heat flow. However, this can be

* Corresponding author. Fax: +1 203 4324283; e-mail: mitanua@minerva.cis.yale.edu.
[1] Present address: NIST, Boulder, CO-80303, USA.
[2] Present address: Department of Electrical Engineering, Ohio State University, USA.


*PII* S0039-6028(96)00464-5

made negligible by choosing an appropriate sample geometry.

## 2. Sample description

The 2DEG devices in a standard Hall configuration were fabricated from modulation-doped, MBE-grown $Al_{0.3}Ga_{0.7}As/GaAs$ heterojunctions. The results presented here were obtained from three different samples fabricated from two wafers, A and B. Table 1 summarizes the sample parameters and geometries. The relevant length scales in the experiment, such as the mean free path and the phase coherence length, are much less than the sample dimensions and the distance between measuring probes. Thus we have a 2D diffusive system and even in the presence of uniform heating, one has a well-defined local electron temperature. For both the samples, it was confirmed using Shubnikov–de Haas measurements that only the first subband is occupied.

## 3. Thermometry

We employ two techniques to determine the electron temperature $T_e$. These give results which are consistent with each other. The first method uses weak localization. The magnetoresistance can be fit to a well established theory [4] to find the electron phase coherence length $L_\phi$. A temperature dependence of $L_\phi \propto T_e^{-1/2}$ is expected to hold down to mK temperatures. The details have been discussed previously [5].

The second method uses the temperature-dependent resistance of the sample, which is primarily due to electron–electron interaction. This is done at a magnetic field large enough to destroy the weak localization. Fig. 1 shows the change in the normalized sample resistance as a function of the mixing chamber temperature for two different measuring currents, 2 and 20 nA (the solid lines are an aid to the eye). The two curves are identical in the high temperature region, while at lower temperatures the curve for 20 nA saturates at a lower resistance value. The curve for 2 nA can thus be used to obtain the temperature of the electron gas when larger currents are used.

Table 1
Sample parameters

| | Sample | | |
|---|---|---|---|
| | A | B1 | B2 |
| $n_s$ ($10^{15}$ m$^{-2}$) | 1.6 | 8.3 | 8.3 |
| $\mu$ (m$^2$/Vs) | 12.4 | 2.3 | 2.3 |
| Number of squares | 20 | 15 | 15 |
| $A$ (mm$^2$) | 0.2 | 0.5 | 0.05 |

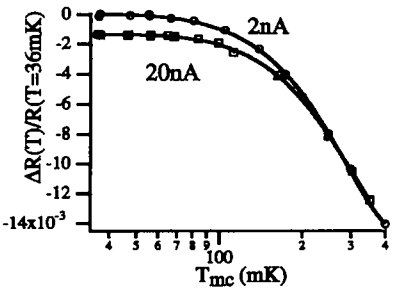


Fig. 1. Change in the normalized resistance of sample B1 as a function of the mixing chamber temperature for two different input currents.

## 4. Theory

At low temperatures, even small power levels can raise the electron temperature above that of the phonons. This temperature difference is determined by the rate at which heat flows out of the electrons to the phonons. There are two different mechanisms for electrons to lose this energy. Hot electrons can relax to lower temperatures via phonon emission. We estimate the power flowing out by this mechanism by a theory put forward by Price [6], which predicts

$$P_{e\text{-}ph} \approx 3.3 \times 10^6 n_s^{-1/2} A_{device}(T_e^5 - T_{ph}^5), \quad (1)$$

in SI units. The numerical factors are valid specifically for a single-subband $Al_{0.3}Ga_{0.7}As/GaAs$ heterojunction. The temperature dependence in Eq. (1) stems from piezoelectric coupling of acoustic phonons to electrons. The electron–phonon coupling due to deformation potential instead has

a $T^7$ temperature dependence. Below 1 K, the power flowing out via this mechanism can be neglected. It should be noted that the existing theories [6,7] do not take into account the effects of impurities of the electron–phonon interaction.

The second mechanism of energy escape is via electron diffusion. Hot electrons can diffuse out to the cold ohmic contacts to be replaced by cold electrons. Using the Wiedemann–Franz law, we calculate the heat flow out through the electron gas (in SI) for our sample geometry to be

$$P_{e\text{-diff}} \approx \frac{10^{-7}}{R}(T_e^2 - T_{ph}^2), \tag{2}$$

where $R$ is the total electrical resistance of the 2DEG between current contacts. Numerical estimates of the thermal conduction path between the sample and the mixing chamber show that the sample lattice and the ohmic contacts are at most 1 mK above the mixing chamber temperature [5].

Fig. 2 depicts the relative importance of the two mechanisms for typical sample parameters. As can be seen, 100 mK represents a rough crossover between the two mechanisms, with electron–phonon coupling dominating at higher temperatures. The dark solid line is the sum of the two contributions and represents the total power flowing out of the electron gas at that temperature.

When heat flows out mainly via electron diffusion, the electrons in the center of the Hall bar are hotter than those near the ohmic contacts. We have simulated the temperature profile along the sample length, including both mechanisms of

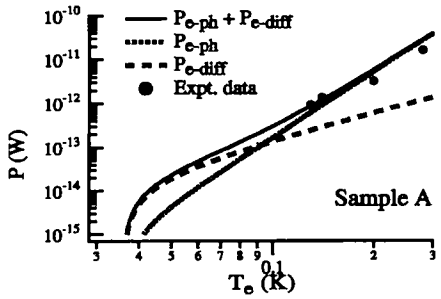


Fig. 2. The power flowing out of the electron gas as a function of the electron temperature at a mixing chamber temperature of 36 mK. The lines are theoretical curves and the dots experimental data.

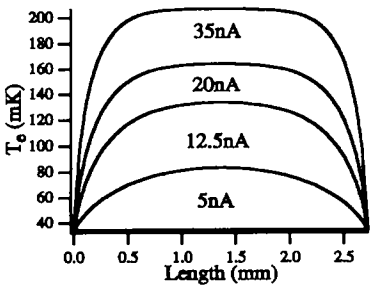


Fig. 3. Simulation of temperature profile along the length of the sample for typical parameters.

heat conduction (Fig. 3). As the input current increases, more heat is carried out by phonon emission and the electrons start to attain a uniform temperature along the sample length. Even when the dominant mechanism of heat flow is electron out-diffusion, the temperature profile is flat near the center. Hence we measure the central region of our sample, which corresponds to the temperature $T_e$ in our formulae.

## 5. Results and discussion

Using Joule heating from the measuring current we dissipate known amounts of power such that in the operating regime, phonon emission is the dominant energy relaxation mechanism. We then determine the electron temperature. The power levels used exceed any extraneous power in the device. Fig. 2 shows the results for sample A. The experimental data is in fair agreement with the theory, confirming that the power flowing out via phonon emission is proportional to $T_e^5$. We can now extract the electron–phonon scattering rate using

$$\tau_{e\text{-ph}}^{-1} = \left(\frac{dP_{e\text{-ph}}/dT_e}{C_e}\right), \tag{3}$$

where $dP_{e\text{-ph}}/dT$ is the thermal conductance due to phonon emission, and $C_e$ the electronic heat capacity for the 2DEG at $T_e$. Hence for sample A we extract $\tau_{e\text{-ph}}^{-1} \approx 2.4 \times 10^8 T_e^3\ s^{-1}\ K^{-3}$. This value, along with the Price prediction, is listed in Table 2. We note that Wennberg et al. [8] used a multiple quantum well heterostructure and found the scat-

Table 2
Electron–phonon scattering rates for samples as predicted by the Price theory and from experiments, and their transport mean free path

| Sample | $\tau_{e-ph}^{-1}/10^8 T^3$ ($s^{-1} K^{-3}$) | | $l$ ($\mu$m) |
|---|---|---|---|
| | Theory | Experiment | |
| A | 3.8 | 2.4 | 0.82 |
| B1 | 1.67 | 9.3 | 0.34 |
| B2 | 1.67 | 10.8 | 0.34 |

tering rate to be two orders of magnitude lower than that predicted by Price.

In order to understand the role of impurities, we fabricated two devices (B1 and B2) from a wafer with lower mobility. They were designed to have the same number of squares and a sheet resistance close to that of sample A ($\approx 315\ \Omega$), ensuring that the thermal conductance due to electron diffusion is similar for all three samples. Samples B1 and B2 are on the same chip and were measured simultaneously, ensuring a comparison based solely on the geometrical difference between the two. Fig. 4 shows the results for samples B1 and B2. The power scales with the device area, implying that phonon emission is the operative energy relaxation mechanism (the power flowing out via electron diffusion is independent of area). We find for both the B devices that the power flowing out per unit area via phonon emission at a given electron temperature is about six times higher than that predicted by Price. Using Eq. (3), we extract an average value of the electron–phonon scattering rate for samples B1 and B2 to be $10^9 T_e^3\ s^{-1}\ K^{-3}$. Thus it appears that the electron–phonon scattering rate increases with disorder.

The electron momentum is uncertain by an amount of order $\hbar/l$, where $l$ is the electron mean free path. Thus, a smaller mean free path leads to an increased phase space for scattered states, and hence a higher scattering rate. To our knowledge, there are no predictions for the dependence of the scattering rate *on disorder* for a 2DEG. A few theories [9–12] do examine this effect in metallic films, but do not reach consensus. We find (Table 2) rough agreement with Takayama's [9] prediction of $\tau_{e-ph}^{-1} \propto l^{-1}$, but this may be fortuitous. Further experiments are in progress.

## 6. Conclusions

We have measured the electron–phonon energy relaxation rates in a 2DEG below 0.5 K. We find a temperature dependence proportional to $T_e^3$ in all our samples. The magnitude is in good agreement with the Price prediction for the cleaner sample, and scales roughly inversely with the mean free path.

## Acknowledgements

The masks were fabricated at NNF, Cornell. Research was supported under NSF DMR 9112752 and AST 9320387.

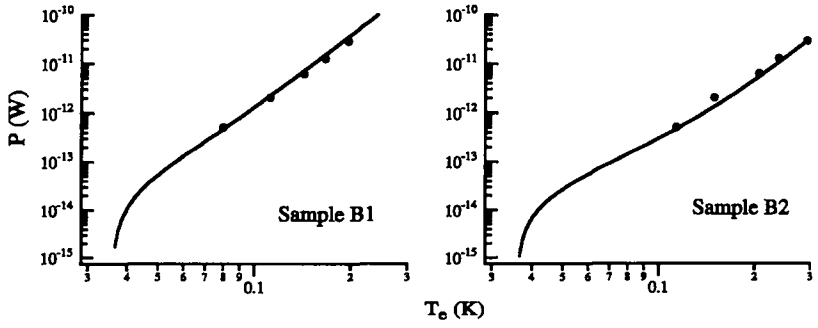


Fig. 4. The total power flowing out of the electron gas versus its peak temperature at $T_{mc} = 36$ mK. The solid lines represent the sum of the heat carried by the Price mechanism multiplied by a factor of six, plus the Wiedemann–Franz contribution.

## References

[1] G. Bergmann, W. Wei, Y. Zhou and R.M. Mueller, Phys. Rev. B 41 (1990) 7386.
[2] G. Bergmann, Phys. Rep. 107 (1984) 1.
[3] P. Santhanam, S. Wind and D.E. Prober, Phys. Rev. B 35 (1987) 3188.
[4] S. Hikami, A.I. Larkin and Y. Nagaoka, Prog. Theor. Phys. 63 (1980) 707.
[5] A. Mittal, M.W. Keller, R.G. Wheeler, D.E. Prober and R.N. Sacks, Physica B 194 (1994) 167. This paper considered only cooling by electron out-diffusion, and thus does not give a complete picture of the heat flow.
[6] P.J. Price, J. Appl. Phys. 53 (1982) 6863.
[7] V. Karpus, Sov. Phys. Semicond. 22 (1988) 268.
[8] A.K.M. Wennberg, S.N. Ytterboe, C.M. Gould, H.M. Bozler, J. Klem and H. Morkoc, Phys. Rev. B 34 (1986) 4409.
[9] H. Takayama, Z. Phys. 259 (1973) 421.
[10] J. Rammer and A. Schmid, Phys. Rev. B 4 (1986) 1352.
[11] M.Y. Reizer and A.V. Sergeyev, Sov. Phys. JETP 63 (1986) 616.
[12] D. Belitz and S. Das Sarma, Phys. Rev. B 36 (1987) 7701.